Comparative analysis of the direct sliding-mode torque control strategies of the induction motor

Grzegorz Tarchała, Teresa Orłowska-Kowalska
Wroclaw University of Technology
50-372 Wrocław, ul. Smoluchowskiego 19, e-mail: {grzegorz.tarchala; teresa.orlowska-kowalska}@pwr.wroc.pl

The paper deals with the sliding-mode torque control of induction motor drives. Two possible control strategies are presented, with stator and with rotor flux stabilization. Mathematical model of the considered drive system and control algorithm is presented. Simulation and experimental results are demonstrated to verify the described algorithms.

1. Introduction

A number of requirements are set to modern electric drives. Superb dynamic behaviour, dependable work, low cost, high power efficiency, motor parameters mismatch insensitivity, simple technical implementation are among the demands. High efficiency, dependable work and low cost can be assured by the usage of an induction motor (IM). However, quite complicated control systems must be applied in order to achieve excellent dynamic transients. This paper presents the Direct Torque Sliding-Mode Control (DTSMC), one of possible ways of controlling the induction motor drive.

Sliding-mode control systems as one of variable structure systems (VSS) have been investigated in Russia from early 1930s [15]. However, first IM drive applications appeared at the turn of 1970s and 1980s as a result of Sabanovic and Izosimov works [3], [11], [12]. The following years achievements enriched the IM Sliding-Mode Control theory, among them are the important Utkin's paper [14], the one considering position control [16] and others, [10], [18]. The subject appears to be still unexhausted and in recent years many new articles have appeared. Authors in [9] proposed a novel SMC algorithm optimizing torque response and efficiency. Conventional DTC and sliding-modes are combined in [6]. Integral nested SM controller is applied to IM in [8], [17] also for sensorless drives [1], [2]. Low and zero-speed action is concerned in [4], [9]. The exponential approach law is introduced in [13]. Second order sliding-mode, so called twisting algorithm, can be also used in IM drives [19].

This paper presents conventional Direct Torque Control taking advantage of sliding-modes, however it compares two possible control strategies assuring motor flux stabilization. Both stator and rotor fluxes can be stabilized, and these two possibilities are investigated and compared. The similarities and differences

between those two methods are shown. Simulation and experimental results are presented to verify the analyzed algorithms.

2. The control strategy – theoretical basics

In order to control a specific plant, like the induction motor drive, the control basics for the general plant should now be introduced. The SMC, as one of the algorithmic control strategies, requires the plant mathematical model knowledge. This model can be described by the commonly-known state equation:

$$\dot{\mathbf{x}} = f(\mathbf{x},\mathbf{k}) \tag{1}$$

where: **x**, **k** – state variables and control signal vectors. The letter **k** appears here to distinguish the common control signal symbol from the motor voltage vector signal **u**.

The next step in the control algorithm design [14] is to choose so-called switching function vector, which can be formulated as:

$$\mathbf{s} = [s_1, s_2, ..., s_N]^T \tag{2}$$

where: N – the number of available control signals.

If the vector **s** is chosen so that its desired value is zero, the negative value of the derivative of the positive Lapunov function ensures the asymptotic convergence of switching function vector. The Lapunov standard function takes the form:

$$L = \frac{1}{2}\mathbf{s}^T\mathbf{s} > 0 \tag{3}$$

and its derivative:

$$\dot{L} = \mathbf{s}^T\dot{\mathbf{s}} < 0 \tag{4}$$

It is important, at this point, to divide the derivative (4) into two parts, one dependent and one independent on the control signal, **k**:

$$\dot{L} = \mathbf{s}^T(\mathbf{f} + \mathbf{D}\mathbf{k}) \tag{5}$$

If the control law is assumed:

$$\mathbf{k} = -\text{sign}(\mathbf{s}^*)^T,\ \mathbf{s}^* = \mathbf{s}^T\mathbf{D} \tag{6}$$

the Lapunov function derivative can be expressed as follows:

$$\dot{L} = \mathbf{s}^T\mathbf{f} - \mathbf{s}^*\,\text{sign}(\mathbf{s}^*)^T = \mathbf{s}^T\mathbf{f} - |\mathbf{s}^*| \tag{7}$$

where: $|\mathbf{s}^*| = |s^*(1)| + |s^*(2)| + |s^*(3)| \geq 0$.

If the term $|\mathbf{s}^*|$ is high enough, the control purpose, i.e. zero convergence of switching functions (2) is fulfilled:

$$\begin{aligned} &\mathbf{s}^T\mathbf{f} - |\mathbf{s}^*| = \mathbf{s}^T\mathbf{f} - |\mathbf{s}^T\mathbf{D}| < 0 \\ &|\mathbf{f}\,\mathbf{D}^{-1}| < 1 \end{aligned} \tag{8}$$

The control law (6), with the usage of the *sign* function, means that the control signals $\mathbf{k}=[k_1,k_2,...k_N]^T$ will only take two signal states, i.e. ±1. This situation,

natural for the modern induction motor drives fed from the voltage-source inverter, will be described in next paragraph.

3. Mathematical model of the converter-supplied induction motor

The power supply chain, commonly found in industrial applications consists of the rectifier, the voltage-source inverter (VSI) and the induction motor. These three elements are presented in Fig. 1.

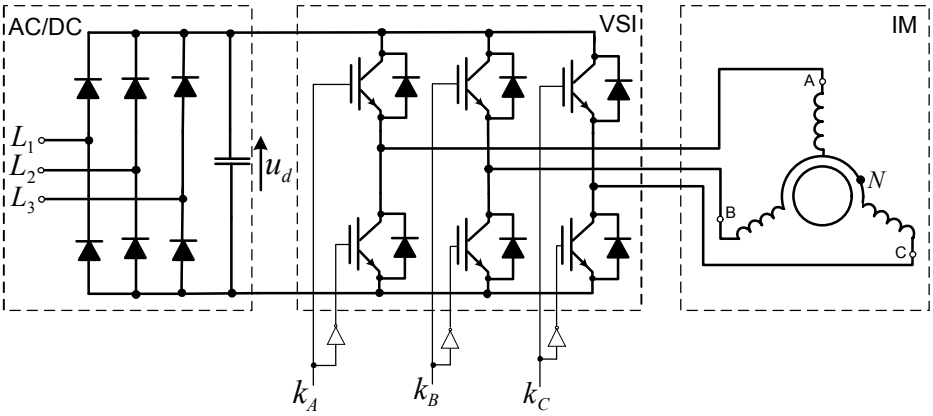

Fig. 1. The induction motor fed from the voltage-source inverter

The rectifier converts the alternating current (AC) into a direct current (DC) and the u_d signal can be assumed as its output. This signal needs to be measured, when the phase voltage values are needed:

$$\begin{bmatrix} u_{AN} \\ u_{BN} \\ u_{CN} \end{bmatrix} = \mathbf{T}_{ABC} \begin{bmatrix} k_A \\ k_B \\ k_C \end{bmatrix} = \frac{u_d}{3} \begin{bmatrix} 2 & -1 & -1 \\ -1 & 2 & -1 \\ -1 & -1 & 2 \end{bmatrix} \begin{bmatrix} k_A \\ k_B \\ k_C \end{bmatrix} \tag{9}$$

where: $\mathbf{k}=[k_A,k_B,k_C]^{\mathrm{T}}$ – the VSI control signals, that become *1* when the specific phase is connected to the positive voltage, and *-1* otherwise.

The conventional induction motor mathematical model will be developed using voltage vector in the stationary reference frame:

$$\begin{bmatrix} u_{s\alpha} \\ u_{s\beta} \end{bmatrix} = \mathbf{T}_{\alpha\beta} \begin{bmatrix} u_{AN} \\ u_{BN} \\ u_{CN} \end{bmatrix} = \frac{2}{3} \begin{bmatrix} 1 & -1/2 & -1/2 \\ 0 & \sqrt{3}/2 & -\sqrt{3}/2 \end{bmatrix} \begin{bmatrix} u_{AN} \\ u_{BN} \\ u_{CN} \end{bmatrix} \tag{10}$$

When the SMC algorithm is concerned another matrix is essential:

$$\mathbf{T} = \mathbf{T}_{ABC}\mathbf{T}_{\alpha\beta} \tag{11}$$

The last part of the presented power supply chain is the squirrel-cage induction motor, which can be described using the well-known space-vector equations expressed in the stationary frame and per unit [p.u.] system [7]:
– voltage and flux equations:

$$\begin{aligned} \mathbf{u_s} &= r_s \mathbf{i_s} + T_N \frac{d}{dt}\boldsymbol{\psi}_\mathbf{s} \\ \mathbf{0} &= r_r \mathbf{i_r} + T_N \frac{d}{dt}\boldsymbol{\psi}_\mathbf{r} - j\omega_m \boldsymbol{\psi}_\mathbf{r} \\ \boldsymbol{\psi}_\mathbf{s} &= x_s \mathbf{i_s} + x_m \mathbf{i_r} \\ \boldsymbol{\psi}_\mathbf{r} &= x_r \mathbf{i_r} + x_m \mathbf{i_s} \end{aligned} \tag{12}$$

– equation of motion:

$$\begin{aligned} \frac{d\omega_m}{dt} &= \frac{1}{T_M}\left(m_e - m_o\right) \\ m_e &= \mathrm{Im}(\boldsymbol{\psi}_\mathbf{s}^* \mathbf{i_s}) = \psi_{s\alpha} i_{s\beta} - \psi_{s\beta} i_{s\alpha} \end{aligned} \tag{13}$$

where:
$\mathbf{u_s} = u_{s\alpha} + j u_{s\beta}, \mathbf{i_s} = i_{s\alpha} + j i_{s\beta}, \boldsymbol{\psi}_\mathbf{s} = \psi_{s\alpha} + j\psi_{s\beta}, \mathbf{i_r} = i_{r\alpha} + j i_{r\beta}, \boldsymbol{\psi}_\mathbf{r} = \psi_{r\alpha} + j\psi_{r\beta}$ – space vectors of stator voltage, current and flux, rotor flux and current, respectively, $r_s, x_s, r_r, x_r, x_m, T_M$ – induction motor parameters, stator and rotor winding resistances, reactances, magnetizing reactance and mechanical time constant, ω_m, m_e, m_o – motor speed and torque, load torque, respectively, $T_N = 1/(2\pi f_{sN}), f_{sN} = 50Hz, \sigma = 1 - x_m^2 / x_s x_r$.

4. SMC application to induction motor drives

Taking into consideration the SMC algorithm presented in paragraph 2, the first step – the deriving of the specific plant mathematical model is now finished, and presented in previous paragraph.

The second step – the switching functions selection must be now considered [5]. There are three control signals, therefore three switching functions are available:

$$\mathbf{s} = \left[s_1, s_2, s_3\right]^T \tag{14}$$

Although sliding-mode theory allows to control motor position, speed or its torque, the goal of this paper is to control the last of them, and thus the first switching function is:

$$s_1 = m_e^{ref} - m_e \tag{15}$$

where: m_e^{ref} – torque reference value.

The motor can be controlled using the constant flux strategy, so the second switching function must be related to the flux; it can be both stator or rotor flux:

$$\begin{aligned} s_{2s} &= (\psi_s^{ref})^2 - \psi_s^2 \\ s_{2r} &= \left(\psi_r^{ref} - \psi_r\right) + T_\psi \frac{d}{dt}\left(\psi_r^{ref} - \psi_r\right) \end{aligned} \tag{16}$$

where: T_ψ – flux control time constant, ψ_s^{ref}, ψ_r^{ref} – stator and rotor flux reference values.

The third and last switching function can be the one providing the 3-phase voltage symmetry:

$$s_3 = \int \left(k_A + k_B + k_C\right) dt \tag{17}$$

For these switching functions the matrix **D**, necessary in the SMC control law application (6) is as follows:

$$\mathbf{D} = \begin{bmatrix} \mathbf{D}_{1s,r} \\ 1 \quad 1 \quad 1 \end{bmatrix} \tag{18}$$

and:

$$\begin{aligned} \mathbf{D}_{1s} &= \frac{1}{T_N} \begin{bmatrix} -2\psi_{s\alpha} & -2\psi_{s\beta} \\ i_{s\beta} - \dfrac{1}{x_s \sigma}\psi_{s\beta} & -i_{s\alpha} + \dfrac{1}{x_s \sigma}\psi_{s\alpha} \end{bmatrix} \mathbf{T} \\ \mathbf{D}_{1r} &= \frac{x_m}{x_r x_s \sigma} \frac{1}{T_N} \begin{bmatrix} -r_r \dfrac{T_\psi}{T_N} \dfrac{\psi_{r\alpha}}{\psi_r} & -r_r \dfrac{T_\psi}{T_N} \dfrac{\psi_{r\beta}}{\psi_r} \\ \psi_{r\beta} & -\psi_{r\alpha} \end{bmatrix} \mathbf{T} \end{aligned} \tag{19}$$

where: $\psi_r = \sqrt{\psi_{r\alpha}^2 + \psi_{r\beta}^2}$ – rotor flux amplitude.

Matrices $\mathbf{D_{1s}}$, $\mathbf{D_{1r}}$ can be obtained substituting (15)-(17) into Lapunov derivative equation (4), (5). The **f** vectors, reminding after dividing the derivative of **s** into two parts (5) are presented in the Appendix 1.

The second switching function forms (16) directly depend on the above-mentioned division to **f** and **D** matrices. The s_{2s} form without raising to the power of two, and the s_{2r} form without the differential part do not allow to realize this division, and thus the **D** matrix cannot be derived.

The block diagram of the SMC structure for IM drive is presented in Fig. 2. The sliding-mode controller, relying on the information of the flux and torque errors, flux vector components (or its amplitude and angle), and additionally stator current vector, changes the control signals, i.e. transistor switches. Fluxes and torque can be calculated by one of many existing estimators [7] using the information about motor phase currents, voltages and speed. The phase voltages are calculated by (9)-(10), taking the advantage of u_d and k_A, k_B, k_C. When there is a necessity of

achieving speeds greater than the nominal value, the field weakening strategy must be applied.

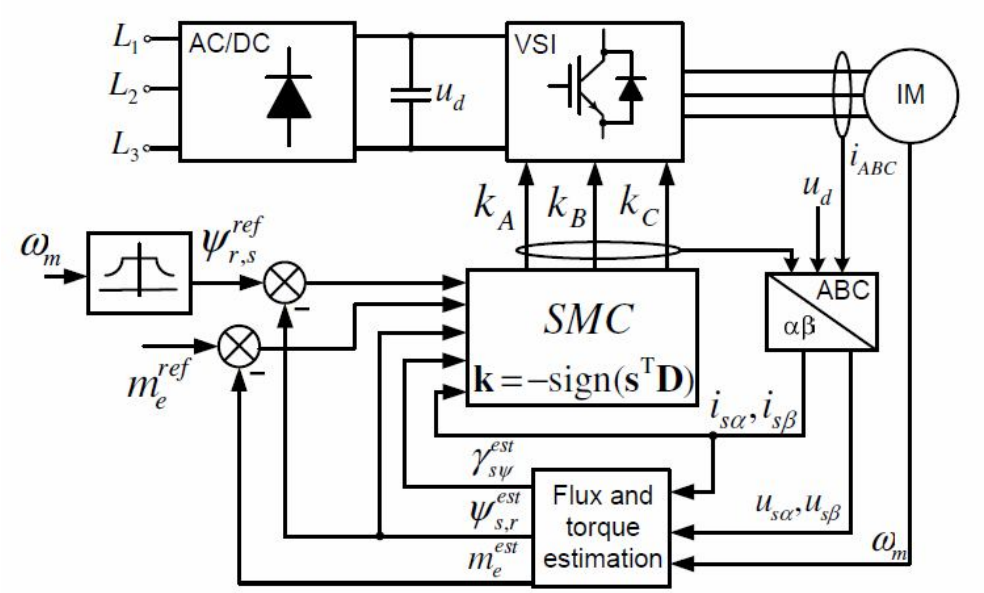

Fig. 2. The block diagram of the direct torque SMC structure

5. Simulation results

Presented above theoretical considerations are proved with simulation tests. All transients are obtained using the Matlab/Simulink software, with the fixed-step Euler method, the sampling time is 1e-6 s. The rectifier and the VSI are assumed to be ideal, i.e. the direct voltage u_d is constant and there is no dead-time effect in the VSI operation. The induction motor model is formed using equations (12)-(13). Its parameters and nominal values are presented in Appendix 2. It is assumed that the flux and torque estimator works properly (Fig. 2).

The drive perfect operation for control with constant stator flux is shown in Fig. 3 It can be noticed that the reference motor torque value is achieved almost immediately and stator flux is kept constant on the desired nominal level. The reference torque square wave amplitude is its nominal value (see Appendix 2). Shape of the speed transient is triangular, due to the applied torque signal.

In Fig. 4 the SMC with constant rotor flux can be seen. The reference torque square wave is identical to the previous one. Likewise for the control with constant stator flux, the system dynamic behaviour is distinguished. Three different transients are shown for three different flux settling time constants $T_{s\psi}$: 0.01s, 0.05s and 0.1s (where $T_{\psi s}=3T_{\psi}$). The torque transients differ only at the beginning, and therefore its zoom is shown. The speed transients are almost identical.

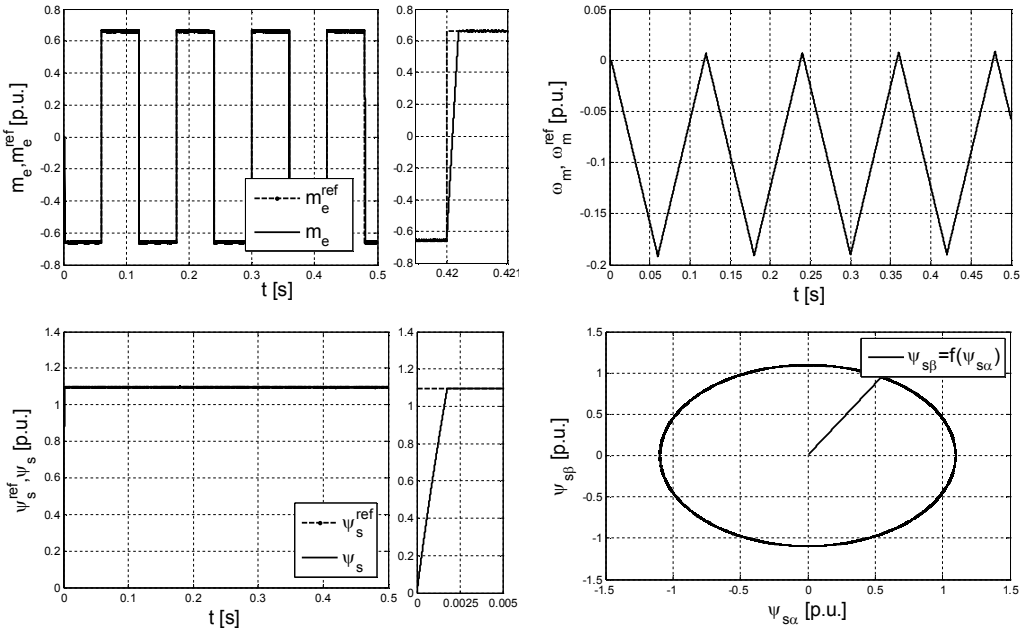

Fig. 3. Sliding-mode control of the induction motor with stator flux stabilization, simulation results

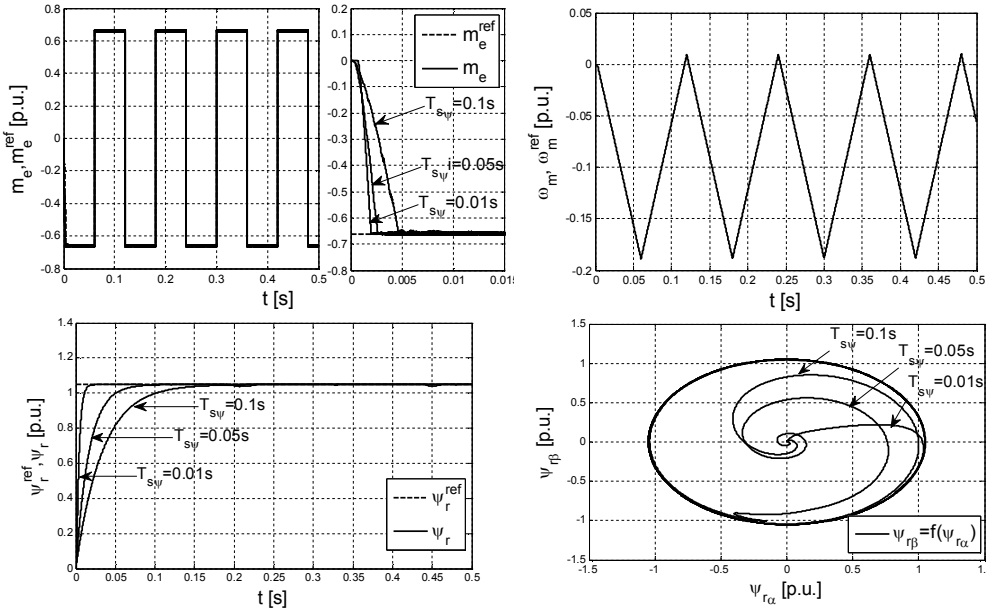

Fig. 4. Sliding-mode control of the induction motor with rotor flux stabilization, simulation results

The parameter sensitivity tests were performed next, and the exemplary transient is shown in Fig. 5. Parameters used by the control system (superscript SMC) were changed in relation to real motor parameters (R). The situation with a parameter mismatch was simulated. Parameters were changed in the following way: $r_s^{SMC} = 2.5 r_s^R$, $x_{s\sigma}^{SMC} = 0.5 x_{s\sigma}^R$, $r_r^{SMC} = 0.5 r_r^R$, $x_{r\sigma}^{SMC} = 2.5 x_{r\sigma}^R$, $x_m^{SMC} = 1.5 x_m^R$. Comparison of the transient from Fig. 5b with the one from Fig. 5a, proves that the SMC algorithm is insensitive to all motor parameters mismatch.

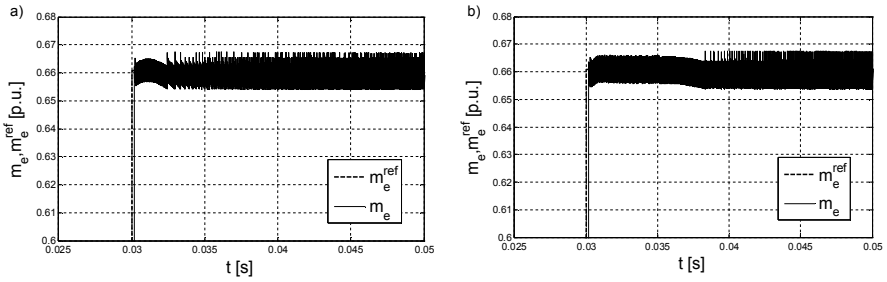

Fig. 5. Parameter sensitivity comparison, a) nominal parameters, b) parameters mismatch: $r_s^{SMC} = 2.5 r_s^R, x_{s\sigma}^{SMC} = 0.5 x_{s\sigma}^R, r_r^{SMC} = 0.5 r_r^R, x_{r\sigma}^{SMC} = 2.5 x_{r\sigma}^R, x_m^{SMC} = 1.5 x_m^R$

6. Experimental results

A number of experimental tests were performed in order to verify presented theoretical considerations. The Sliding-Mode Control algorithms were implemented in dSpace 1104 card using the dSpace software. The tests were performed with the sampling time 60μs. The schematic diagram of a laboratory set-up is presented in Fig. 6.

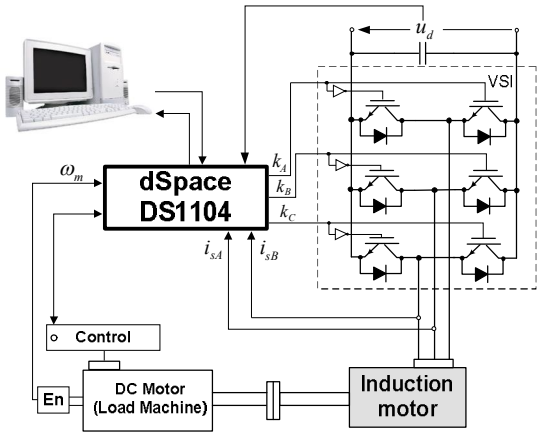

Fig. 6. Experimental set-up

The set-up consists of the 1.5kW induction motor fed from the VSI. The load torque is provided by the DC machine. Whole control process is supervised by the dSpace 1104 card. Motor speed is measured by the incremental encoder (4096 imp./rev.).

Both control methods, with stator and rotor flux stabilization, were tested. Experimental transients for the first method are presented in Fig. 7, for the second method in Fig. 8, respectively. In both cases the flux vectors were estimated by commonly used simulators [7]; the stator flux vector was estimated by the voltage-based simulator and the rotor flux – by the current-based simulator.

Both control methods give almost the same results. In Fig. 7 and Fig. 8 a superb control system performance can be seen. Reference torque values are achieved almost immediately. One of the differences is that rotor flux oscillations are smaller then in stator flux signal. Speed signal is triangular due to the applied motor torque signal shape.

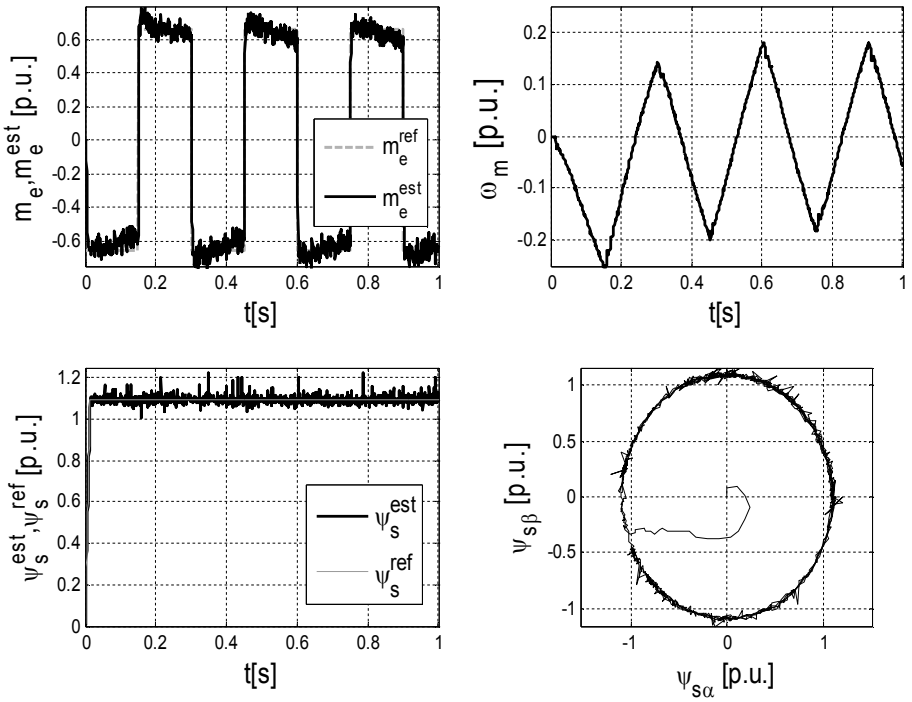

Fig. 7. SMC with stator flux stabilization, experimental results

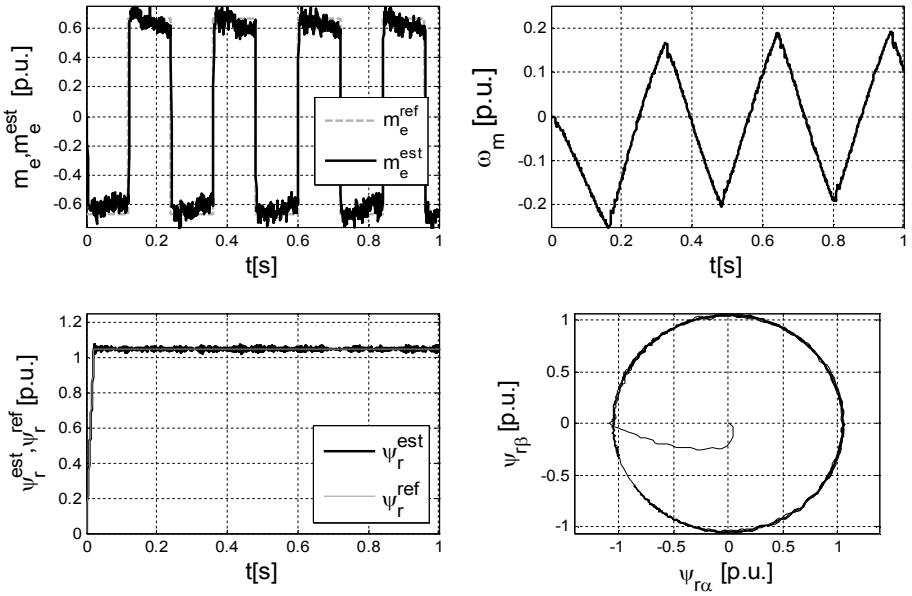

Fig. 8. SMC with rotor flux stabilization, experimental results

7. Conclusion

In the paper the Direct Torque Sliding Mode Control is presented. The two possible control strategies are compared – one that allows to keep stator flux constant and the second one for rotor flux. Simulation and experimental test were performed to verify described algorithms. Both control strategies give almost the same results – motor torque is controlled ideally, the reference value is achieved almost immediately and the flux is kept constant. The only difference, noticeable during experimental tests, are smaller flux oscillation for drive system operation with stabilisation of the rotor flux.

Appendix 1

The **f** vectors reminding after the derivative of **s** division (5) will be presented here, respectively for constant stator flux control:

$$\begin{bmatrix} f_{1s} \\ f_{2s} \end{bmatrix} = \begin{bmatrix} \dot{m}_e^{ref} - \frac{1}{T_N}\left[\omega_m\left(i_{s\alpha}\psi_{s\alpha} + i_{s\beta}\psi_{s\beta}\right) - \frac{1}{x_s\sigma}\left(\left(-r_s + \frac{r_r x_s}{x_r}\right)m_e + \omega_m\psi_s^2\right)\right] \\ 2\psi_s^{ref}\dot{\psi}_s^{ref} + \frac{2r_s}{T_N}\left(i_{s\alpha}\psi_{r\alpha} + i_{s\beta}\psi_{r\beta}\right) \end{bmatrix} \quad \text{(A1)}$$

and for control with constant rotor flux:

$$\begin{bmatrix} f_{1r} \\ f_{2r} \end{bmatrix} =$$

$$\begin{bmatrix} f_{1r} = \dfrac{1}{T_N}\left[-\dfrac{r_s x_r + r_r x_s}{x_r x_s \sigma} m_e - \omega_m \dfrac{x_m}{x_r}\left\{ \left(\psi_{r\alpha} i_{s\alpha} + \psi_{r\beta} i_{s\beta} \right) + \dfrac{x_m}{x_r x_s \sigma} \psi_r^2 \right\} \right] \\ \dot{\psi}_r^{ref} + T_\psi \ddot{\psi}_r^{ref} - \dfrac{T_\psi}{\psi_r T_N} \dfrac{r_r}{x_r} \left(-\dfrac{1}{2} \dfrac{r_r x_m^2}{x_r} \dfrac{p^2}{\psi_r^2} + a_1 \psi_r^2 + \dfrac{1}{T_N} \dfrac{r_r x_m^2}{x_r} \left(i_{s\alpha}^2 + i_{s\beta}^2 \right) + a_2 p - \dfrac{3x_r}{T_N} \omega_m m_e \right) \end{bmatrix}$$

where:

$$a_1 = \left(-\frac{1}{2}\frac{r_r}{x_r} + \frac{1}{T_\psi} + \frac{1}{T_N}\left(\frac{r_r}{x_r} + \frac{x_m}{x_s \sigma}\left(\frac{r_r x_m}{x_r^2} + 1 \right) \right) \right), a_2 = \left(-\frac{x_m r_r}{2x_r} + \frac{x_m}{T_\psi} - \frac{1}{T_N}\left(\frac{2x_m r_r}{x_r} + \frac{x_m}{x_s \sigma}\left(r_s + r_r \frac{x_m^2}{x_r^2} + x_m \right) \right) \right)$$

Appendix 2

Induction motor (Indukta Sh90 L-4) parameters and its nominal values are presented in Table 1 and Table 2, respectively.

Table 1. Parameters of the IM equivalent circuit

R_s	R_r	X_s	X_r	X_m	
4.8431	6.57	84.9	84.9	81.4	[Ω]
0.0737	0.10	1.29	1.29	1.239	[p.u]

Mechanical time constant of the drive: T_M=0.2s

Table 2. Motor nominal values

Power	Torque	Speed	Voltage	Current	Frequency	Stator flux	Rotor flux	
P_N	M_N	n_N	U_{sN}	I_{sN}	f_{sN}	Ψ_{sN}	Ψ_{rN}	
[kW]	[Nm]	[rpm]	[V]	[A]	[Hz]	[Wb]	[Wb]	[physical units]
1.5	10.2	1410	230	3.5	50	1.135	1.087	
0.62	0.6608	0.94	0.707	0.707	1	1.096	1.049	[p.u.]

References

[1] Comanescu M., An Induction-Motor Speed Estimator Based on Integral Sliding-Mode Current Control, *IEEE Trans. Industrial Electronics,* vol. 56, no. 9, September 2009, pp.3414-3423.

[2] Comanescu M., Xu L., Batzel T.D., Decoupled Current Control of Sensorless Induction-Motor Drives by Integral Sliding Mode, *IEEE Trans. Industrial Electronics,* vol. 55, no. 11, Nov. 2008, pp.3836-3845.

[3] Izosimov D. B., Matic B., et al., Using sliding modes in control of electrical drives, *Dokl. ANSSSR,* vol. 241, no. 4, 1978, pp. 769-772 (in Russian).
[4] Jezernik K., Speed Sensorless Variable Structure Torque Control of Induction Motor, *Proc. of Int. Conf. on Industrial Technology ICIT'2009*, India, 2009.
[5] Kajstura K., Orłowska-Kowalska T., Sliding-mode control of induction motor, *Prace Nauk. Inst. Maszyn, Napędów i Pomiarów Elektr. Polit. Wrocł., no. 56, ser. Studia i Materiały*, no. 24, 2004, pp. 279-290 (in Polish).
[6] Lascu C., Trzynadlowski A., Combining the Principles of Sliding Mode, Direct Torque Control and Space-Vector Modulation in a High-Performance Sensorless AC Drive, *IEEE Trans. Industry Applications*, vol. 40, no. 1, January/February 2004, pp.170-177.
[7] Orłowska-Kowalska T., Sensorless Induction Motor Drives, Wroclaw University of Technology Press, 2003 (in Polish).
[8] Rivera J., Loukianov A., Integral Nested Sliding Mode Control: Application to the Induction Motor, *Proc. International Workshop on Variable Structure Systems*, Italy, 2006, pp.110-114.
[9] Rodic M., Jezernik K., Sabanowic A., Speed Sensorless Sliding Mode Torque Control of Induction Motor, *Proc IEEE Industry Applications Conference*, vol.3, Rome, Italy, 2000, pp. 1820-1827.
[10] Sabanovic A., Bilalovic F., Sliding Mode Control of AC Drives. *IEEE Trans. Industrial Applications,* vol. 25, No. 1, January 1989, pp. 70-75.
[11] Sabanovic A., Izosimov D. B, Application of sliding modes to induction motor control, *IEEE Trans. Industry Applications*, vol. IA-17**,** no. 1, January/February 1981, pp. 41-49.
[12] Sabanovic A., Izosimov D. B, Music O., Bilalovic F., Sliding modes in controlled motor drives, *Proc. IFAC Conference on Control in Power Electronics and Electrical Drive*, Lausanne, Switzerland, 1983, pp. 133-138.
[13] Sun D., Sliding Mode Direct Torque Control for Induction Motor with Robust Stator Flux Observer, *Proc. 2010 Int. Conf. on Intelligent Computation Technology and Automation*, China, 2010.
[14] Utkin V., Sliding Mode Control Design Principles and Applications to Electric Drives, *IEEE Trans. Industrial Electronics,* vol.40, no.1, 1993, pp.23-36.
[15] Utkin V., Guldner J., Shijun M., *Sliding mode control in electromechanical systems*, Taylor & Francis, 1999.
[16] Veselic B., Perunicic-Drazenovic B., Milosavljevic C., High-Performance Position Control of Induction Motor Using Discrete-Time Sliding-Mode Control, *IEEE Trans. Industrial Electronics,* vol. 55, no. 11, November 2008, pp.3809-3817.
[17] Wang J., Li C., Li H., The Application of Integral Sliding Mode Variable Structure in Induction Motor Vector Control System, *Proc. 2nd Int. Conf. on Mechanical and Electronics Engineering*, Japan, 2010.
[18] Yan Z., Jin C., Utkin V., Sensorless Sliding-Mode Control of Induction Motors, *IEEE Trans. Industrial Electronics,* vol.47, no.6, 2000, pp.1286-1297.
[19] Zhang Z., Zhu J., Tang R., Bai B., Zhang H., Second Order Sliding Mode Control of Flux and Torque for Induction Motor, *Proc. Asia-Pacific Power and Energy Engineering Conference*, China, 2010.